

## Anisotropic Creep Modeling for f.c.c. Single Crystals

A. BERTRAM, J. OLSCHESKI, M. ZELEWSKI, R. SIEVERT  
Federal Institute for Materials Research and Testing (BAM), Berlin, FRG

### Summary

The one-dimensional behavior of single crystal superalloys at high temperatures under constant and cyclic creep conditions is described by means of a 4-parameter rheological model based on linear viscoelasticity. Tertiary creep is taken into account by reducing the effective cross section by means of an additional damage parameter. Tensile creep tests have been used for the identification of the material constants by a non-linear optimization procedure. For the generalization to three dimensions, a complete tensor-representation of cubic material symmetry is given. It contains twelve (temperature dependent) material parameters. Some results by finite element analysis will be presented.

### Introduction

Within the last decade, single crystal superalloys have become more and more important for blading within the hot section of gas turbines. Because of their f.c.c. crystal structure the material behavior is highly orientation dependent and, hence, must be treated as (cubic) anisotropic. At high temperatures the inelastic properties under constant and cyclic loads are of paramount interest for the design of blades. Creep experiments show us that, after a short phase of primary creep, the secondary or steady creep phase almost immediately turns over into the overlinear phase of tertiary creep. Because of the absence of grain boundaries in single crystals, the creep deformation can reach about 20% so that nonlinear geometrical effects are to be considered at that stage, although the physical nonlinearities due to creep damage are predominant.

### One-dimensional theory

As starting point for our analysis we choose a four-parameter model from linear viscoelasticity which consists of two elasticities and two viscosities (Fig.1). The governing differential equation in the stress  $\sigma$  and the tension  $\epsilon$  which completely describes the behavior of the model is

$$\sigma'' + a_1 \sigma' + a_2 \sigma = a_3 \epsilon'' + a_4 \epsilon', \quad (1)$$

where the four (positive) material constants are given by

$$a_1 = C/D + C/L + K/L, \quad a_2 = (CK)/(L.D), \quad a_3 = C + K, \quad a_4 = CK/D \quad (2)$$

International Union of Theoretical  
and Applied Mechanics

M. Życzkowski (Ed.)

# Creep in Structures

4th IUTAM Symposium, Cracow, Poland  
September 10-14, 1990

Springer-Verlag  
Berlin Heidelberg New York  
London Paris Tokyo  
Hong Kong Barcelona Budapest

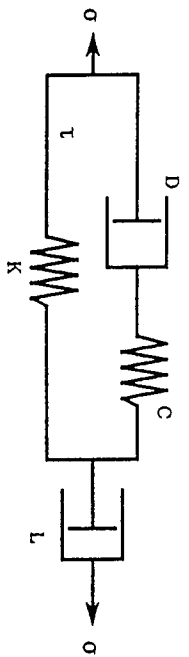


Fig. 1. Rheological model.

By introducing the stress in the lower branch of the model as an internal variable

$$\tau(t) := K \int_0^t \{ \dot{\epsilon}(s) - \sigma(s) / L \} ds \quad (3)$$

we obtain the evolution equations for the model

$$\dot{\tau} = c_1 \sigma' + c_2 (\sigma - \tau) \quad (4)$$

$$\dot{\epsilon} = c_3 \sigma' + c_4 \sigma + c_5 \tau \quad (5)$$

such that the constants  $c_i$  are determined by

$$c_1 = K / (C + K), \quad c_2 = c_1 C / D, \quad c_3 = 1 / (C + K), \quad c_4 = c_3 a_1, \quad c_5 = -c_3 C / D.$$

The two evolution equations (4) are appropriate for numerical integration and may serve for describing the primary and secondary creep behavior in constant and cyclic creep tests as shown in Figs. 2, 3. The asymptotic behavior as  $t \rightarrow \infty$  is linear, being governed by the viscosity  $L$ . Hence the range of this simple model is limited to short creep intervals.

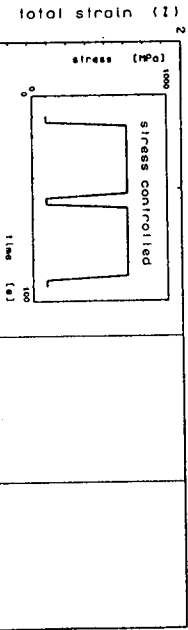


Fig. 2. Cyclic creep with hold times. (dashed line: experiment)

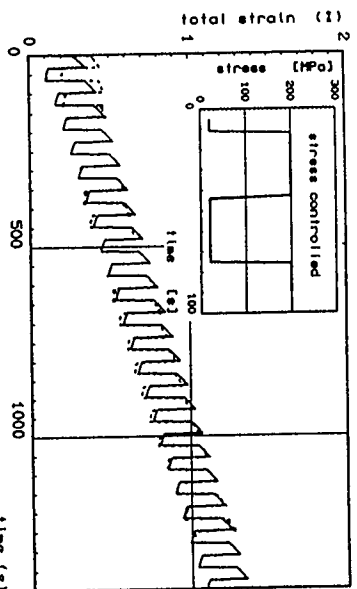


Fig. 3. Cyclic creep with hold times at 980 C.

Damage modeling

If we are interested in the long range creep behavior till final failure, we introduce a damage variable  $\delta$ , which may be interpreted as the loss of effective cross section as suggested by KACHANOV and RABOTNOV (see KRAJCIHOVIC / LEMAITRE [11])

$$A_e = A_0 (1 - \delta), \quad (6)$$

where  $A_0$  is the apparent cross section area,  $A_e$  is the effective (or fictitious) area which initially equals  $A_0$ . However, this is by no means the only interpretation of  $\delta$ . In analogy to (4) we assume the evolution function of the damage parameter

$$\dot{\delta} = c_6 \sigma + c_7 \sigma' + c_8 \tau + c_9 \delta \quad (7)$$

In Fig. 4 a set of experimental results of constant creep tests is plotted. The points of measurements are marked by symbols. All of these tests were performed at a temperature of 760 °C by an INSTRON tensile testing machine on cylindrical samples of the nickel base superalloy SR99 with orientations near to [1 0 0]. Note the large scatter of experimental results at the same stress level, which is typical for creep tests.

As a first step, these data were used to determine the constants in (4) and (7) by a nonlinear optimization technique which minimizes the difference between measured and calculated deformation in each of these points for each test separately. It turned out that the dominant term in (7) is the first one, so that a reduced form

$$\dot{\delta} = c_6 \sigma \quad (8)$$

gives similar results. The curves in Fig. 4 show these calculated creep curves which prove the capability of the model to describe creep behavior in the full range of these tests.

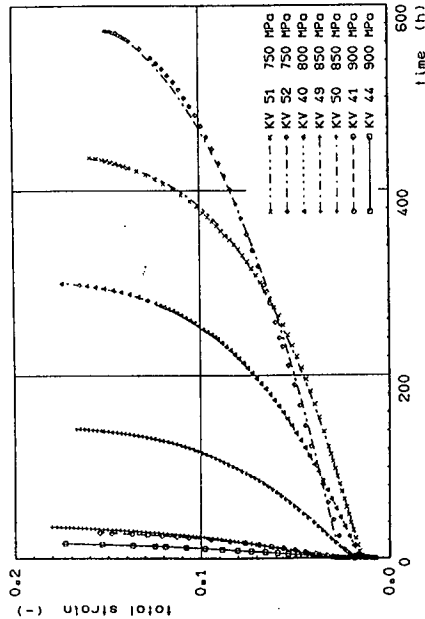


Fig. 4. Creep tests at 760 C. Experiment and calculation.

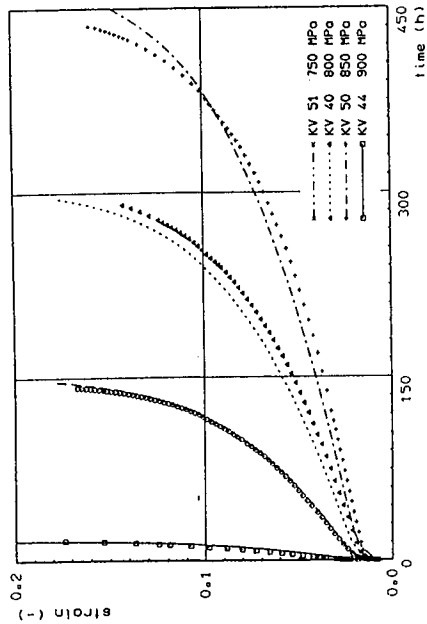


Fig. 5. Global adjustment of creep tests KV51, 40, 44, 50

In order to do a global identification, i. e. to give a single set of material constants that describe all of the creep tests in the given range, we suggest the following procedure. First, select one test as a master curve for the others (in our case we

chose KV51) and identify C, K, D, L, and  $\epsilon_0$  by fitting this single test. Second, introduce a linear time transformation by

$$t^* = t / \alpha \tag{9}$$

where t is the real time,  $t^*$  is an artificial or internal time, and  $\alpha$  is a time scaling factor, that depends on the initial stress  $\sigma_0$ . In our case the linear form

$$\alpha = (k_1 \sigma_0 + k_2) \tag{10}$$

gives satisfying results. We now solve the evolution equations (4) with respect to the internal time  $t^*$  and afterwards transform the solution to the real time by means of (9) and (10). The results are given in Fig.5 together with a selected set of creep tests. The parameter list is given in Table.1.

C	K	D	L,
GPa	GPa	GPa h	GPa h
50.52	49.64	57.69	6775.

$\epsilon_0$	$k_1$	$k_2$
(GPa h) <sup>-1</sup>	(GPa) <sup>-1</sup>	-
1.448	-6.366	5.775

Table 1. Material constants for SRR99 at 760 C

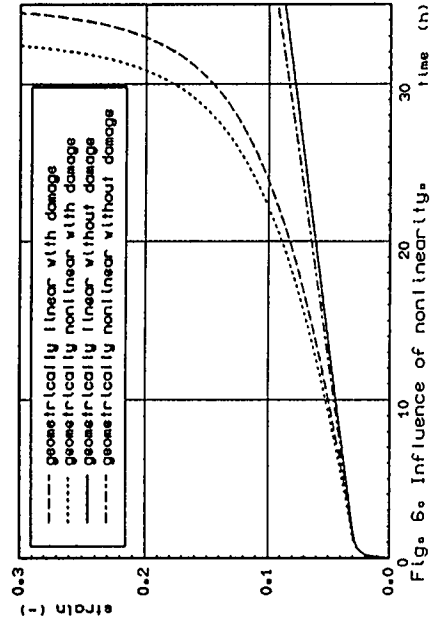


Fig. 6. Influence of nonlinearity.

In order to investigate the influence of geometrical nonlinear effects, a comparison between geometrical linear and nonlinear calculations (assuming isochoric creep deformations) is given in Fig. 6 with and without damage for a single set of material parameters. The difference between the two approaches is remarkable for larger deformations but small if compared with the effect of damage. Thus, we can conclude that the effect of geometrical linearization can be equally included by an appropriate choice of damage constants (as being done in Figs. 4 and 5).

Three-dimensional theory

Three dimensional creep laws are needed not only to predict the creep behavior in arbitrary orientations, but, moreover, for inhomogeneous tests such as on notched bars. In literature only few suggestions have been made to include anisotropy in three-dimensional creep laws (see, e. g., MURAKAMI / SAWCZUK [2], BETTEN [3] and [4]).

We obtain the three-dimensional constitutive model by generalizing the one-dimensional one in analogy to the three-dimensional linear elastic law which is well known since about one century for this crystal class (see VOIGT [5]). In doing so, let the vectors  $e_i$  describe the three orthogonal crystal axes. We introduce three projections (fourth order tensors) by

$$\begin{aligned} P_1 &= \frac{1}{3} I \otimes I \\ P_2 &= I - \sum_i (e_i \otimes e_i \otimes e_i \otimes e_i) \\ P_3 &= I - P_1 - P_2 \end{aligned} \tag{11}$$

Here,  $I$  is the second order identity,  $I$  the fourth order identity, and  $\otimes$  the tensor product. The advantage of these notions is that any linear transformation between symmetric tensors that fulfills cubic anisotropy is a linear combination of these three projections. For example, the cubic form of HOOKE's law is

$$S = C[E] \quad \text{with} \quad C = \sum_i c_i P_i, \tag{12}$$

where  $S$  is the stress tensor and  $E$  the linear strain tensor. If we use linear laws like (12) for each element in our rheological model, we obtain the three dimensional cubic generalization of (1)

$$S'' + A_1[S'] + A_2[S] = A_3[E''] + A_4[E'] \tag{13}$$

where  $A_j, j = 1, \dots, 4$ , are fourth order material tensors and, thus, linear combinations like

$$A_j := d_{1j} P_1 + d_{2j} P_2 + d_{3j} P_3 = \sum_i d_{ij} P_i \tag{14}$$

with

$$\begin{aligned} d_{1i} &= C_i / D_i + C_i / L_i + K_i / L_i, \quad d_{2i} = (C_i K_i) / (L_i D_i), \\ d_{3i} &= C_i + K_i, \quad d_{4i} = C_i K_i / D_i, \quad i = 1, 2, 3 \end{aligned} \tag{15}$$

with  $3 \times 4 = 12$  real constants  $d_{ij}$ . For example, the cubic form of the evolution equation is

$$T'' = \sum_i P_i [f_i S'' + g_i (S - T)] \tag{16}$$

$$E' = \sum_i P_i [h_i S' + p_i S + q_i T].$$

Here  $T$  is the tensor of the internal variables defined by

$$T(t) := \sum_i K_i P_i \left[ \int_0^t \{ E(s) - S(s) / L_i \} ds \right] \tag{17}$$

and the real constants are determined by

$$f_i = K_i / (C_i + K_i), \quad g_i = f_i C_i / D_i, \quad h_i = 1 / (C_i + K_i), \quad p_i = h_i d_{1i}, \quad q_i = -h_i C_i / D_i \tag{18}$$

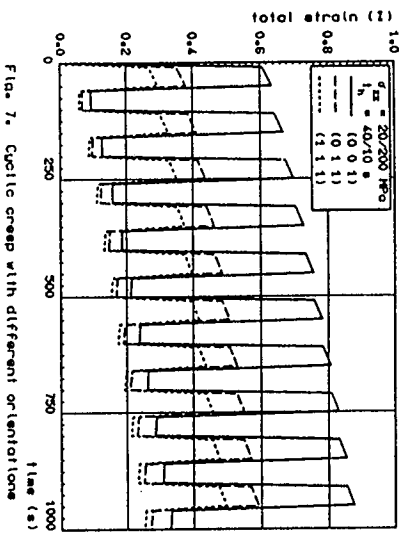


Fig. 7. Cyclic creep with different orientations

It is easy to make (16) explicit in terms of stress increments, if one prefers deformations as independent variables. These versions are appropriate for implementation into finite-element-codes. The results shown in Fig. 7 have been

obtained by using ADINA [6] for tensile cyclic creep test of different orientations. The twelve material constants were only roughly fitted to experimental results. In BERTRAM et al. [7] applications to notched specimens are shown. A three-dimensional version of the damage equation will not be given here.

#### References

1. Krajcinovic, D.; Lemaitre, J.: Continuum damage mechanics. Wien, New York: Springer-Verlag (1987).
2. Murakami, S.; Sawczuk, A.: A unified approach to constitutive equations of inelasticity based on tensor function representations. Nucl. Engn. Des. 65 (1981) 33-47.
3. Betten, J.: Materialgleichungen zur Beschreibung des sekundären und tertiären Kriechverhaltens anisotroper Stoffe. Z. ang. Math. Mech. 64, 6 (1984) 211-220.
4. Betten, J.: Representation of initial and deformation induced anisotropy in creep mechanics. In: Advances in plasticity 1989. Khan, A. S.; Tokuda, M. (eds.) Oxford: Pergamon Press (1989) 677-681.
5. Voigt, W.: Lehrbuch der Kristallphysik. Leipzig, Berlin: Teubner (1910).
6. Bathe, K.-J.: ADINA, a finite element program for automatic dynamic incremental nonlinear analysis. Report AE 84-1. ADINA Eng. Inc., Watertown MA, USA (1984).
7. Bertram, A.; Olschewski, J.; Sievert, R.; Zelewski, M.: Constitutive modeling of the creep behaviour of single crystals with applications to notched specimens. Proc. 3. Int. Conf. Const. Laws for Eng.-Mat., Tucson (1991) (to appear).

#### Acknowledgement

This report was supported by the Bundesminister für Forschung und Technologie under grant 03-M 3005 C4.

